Journal of Structural Geology, Vol. 3, No. 1, pp. 25 to 37, 1981
Printed in Great Britain

0191-8141/81/010025-12 $02.00/0

Brittle deformation in pitted pebble conglomerates

T. J. McEwen

Natural Environmental Research Council, Institute of Geological Sciences,
Building 151, Harwell Laboratory, Harwell, Oxon OX11 0RA, England

(*Received* 15 *August* 1980; *accepted in revised form* 2 *December* 1980)

Abstract—The fracture patterns produced in pitted pebble conglomerates from the Alpine Molasse and the Carboniferous of northern Spain, have been studied in relation to the stress concentrations which were produced in the conglomerates during their deformation. The stress distributions which develop around pebble contacts at different stages of their pitting history have been determined from photoelastic experiments. The development of different types of fracture, having dominantly tensile or shear components, and their distribution within the pebbles, are shown to be related to the mineralogy of the pebbles, the strength of the matrix and the amount of deformation the conglomerate has suffered.

INTRODUCTION

The structures formed by brittle deformations in conglomerates from the Alpine Molasse, the Carboniferous Westphalian B–C–D and Stephanian B in Cantabria and Asturia, and the Bunter of Cannock Chase have been studied in order to relate the types and arrangements of fractures and other brittle features to the deformation the conglomerate has suffered. The conglomerates studied were those where pitting of the pebbles had occurred at their mutual contacts, and where diffusional mass transfer was the dominant deformation mechanism (McEwen 1977, 1978). The conglomerates were all deformed at temperatures of less than 200°C, and the deformation rates were in many cases slow enough to enable the strain to be accommodated mainly in a non-brittle deformation. Although the brittle features of the deformation were in most cases of secondary importance when compared with the diffusive deformation mechanisms, they still played a significant role in the complete deformation.

The effects of brittle deformation can have important consequences on the rates of pebble pitting, on the structures formed at pebble contacts and in the matrix, and on the rates of deformation of the conglomerate.

Photoelastic experiments have been performed in order to discover the changes that occur in the stress distribution when pitting occurs between pebbles. The results from the photoelastic experiments are compared with theoretical predictions on fracture mechanisms and with the naturally occurring examples.

PHOTOELASTIC EXPERIMENTS

Photoelastic experiments were performed in order to calculate the stresses produced during the pitting in deformed conglomerates. Models were made from Araldite Resin C.T. 200 sheet, 6 mm thick (from Sharples Photomechanics Ltd.), and loaded with 45 kg in uniaxial compression. In order to model the progressive solution of one of the pebbles in contact, a disc 7.5 cm in diameter was loaded in turn against five different rectangular blocks (15 cm × 15 cm). From each block a circular segment corresponding to the solution pit at different stages of its development was cut, the diametral depths of the segments being 0.158, 0.317, 0.635, 1.27 and 2.54 cm. The disc was also loaded against an uncut block. During the pitting of pebbles it is commonly observed that only one of the pebbles suffers volume loss — the indenting pebble is often very little affected. The progressive development in two dimensions of a spherical pebble indenting a plane is therefore modelled at six stages during its formation. The tolerance between the disc and the circular segments was $< \pm 2.5 \times 10^{-3}$ cm, and cutting of the Araldite Resin was done extremely carefully so that thermal stressing was minimised. Because of good tolerance between the separate segments in the experiment no lateral support was necessary.

The experiments enabled the following to be calculated:

(a) Isochromatics, lines of equal magnitude of maximum stress difference.
(b) Isoclines, lines of equal orientations of σ_1.
(c) Stress trajectories, trajectories of σ_1 and σ_2.
(d) Slip lines, $\sigma_{zx_{max}}$ trajectories when plane strain is assumed.
(e) Potential shear planes, assuming $\phi = 30°$.
(f) Constant shear stress trajectories, calculated from the Mohr Circle assuming local equilibrium throughout the model.
(g) Separation of the principal stresses along certain lines through the model by the shear difference method (Kuske & Robertson 1974).

Isochromatics

The maximum isochromatic fringe order (the maximum stress difference within the model) decreases rapidly as the contact area increases (Fig. 1). The curve for $(\sigma_{zz} - \sigma_{xx})$ max can be compared with the decrease in

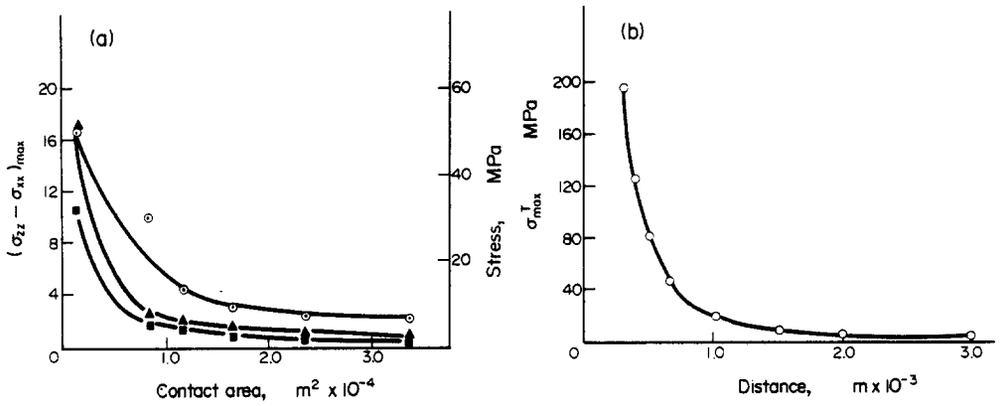

Fig. 1. (a) The maximum isochromatic fringe order (the maximum stress difference within the model) ⊙; the maximum compressive stress on the contact ▲; and the mean compressive stress on the contact ■, plotted against the contact area between the disc and the block. (b) The maximum value of the tensile stress in the surface region of a plane surface, with the same elastic constants as the indenting sphere, due to the Hertzian loading of a sphere (radius 0.005 m, $E = 5.5 \times 10^4$ MPa, $\nu = 0.25$) with load (P) of 250 kg; plotted against the distance from the centre of the contact. Calculated from Hertz (1881) $\sigma T_{max} = \frac{1}{2}(1 - 2\nu)(P/\pi a^2)$ where a is the radius of the contact.

mean compressive stress calculated assuming a constant stress over the contact surface, and the maximum compressive stress on the contact, assuming that the maximum compressive stress = 3/2 (mean compressive stress), as is the case for the Hertzian contact. The maximum stress difference decreases less rapidly than the compressive stress with increase in the contact area; this is because σ_{xx} does not decrease as rapidly as σ_{zz}. For the Hertzian contact the maximum fringe order is in the centre of the contact (Fig. 2a), with increase in contact area the maxima are shifted to the boundaries of the contact zone (Fig. 2b), with no further increase in area the maxima become more diffuse but again in the centre of the contact (Fig. 2c).

Potential shear planes

These are constructed assuming an angle of internal friction (ϕ) of 30°. They are almost symmetrical about the contact area (they should be symmetrical about the loading axis for perfect uniaxial loading) and are initially at high angles to the contact surface (Fig. 3a). With increase in contact area low angle shear planes are produced on the boundaries of the contact, but they still

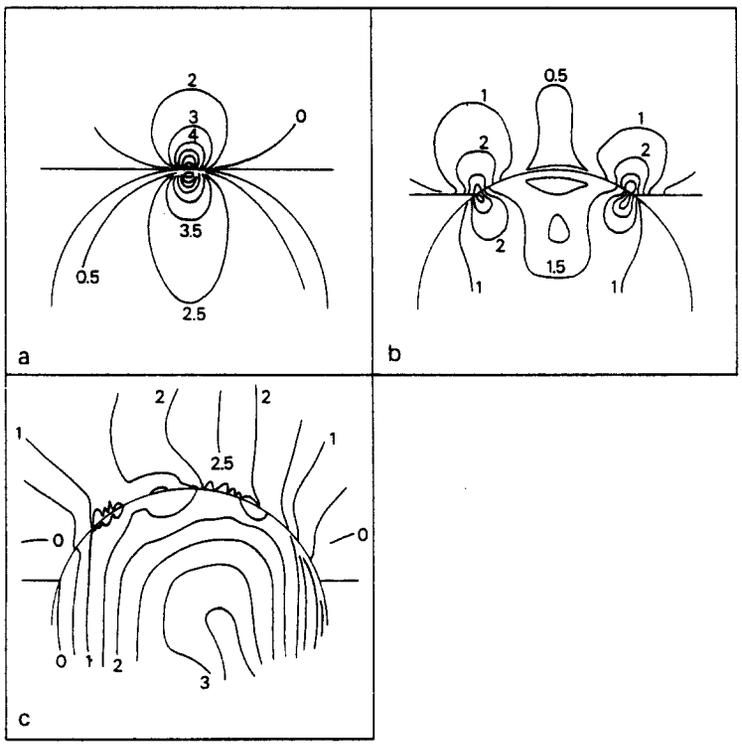

Fig. 2. Isochromatics found from loading a disc against a plane surface (a); a circular cut out of 0.635 cm (b); and a cut out of 2.54 cm (c).

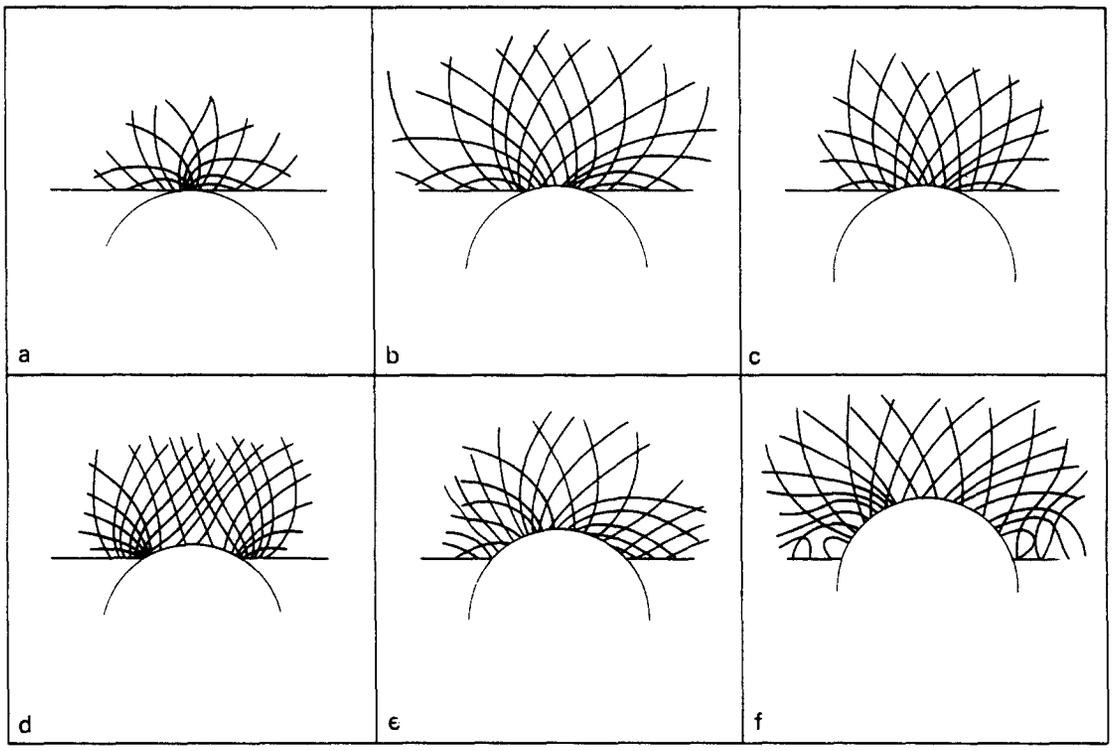

Fig. 3. Potential shear planes developed by the six different loading configurations (detailed in the section entitled Photoelastic experiments), assuming an angle of internal friction (ϕ) of 30°.

remain at high angles in the centre (Figs. 3b–e). In Fig. 3(f) complex zones are developed around the edges of the contact zone.

Trajectories of σ_1 and σ_n

Trajectories of σ_1 and σ_n (the maximum compressive stress and the normal stress on the contact respectively) around the contact are constructed from the stress trajectories and by drawing normals to the contact surface. In the centre and close to the contact, trajectories of σ_1 and σ_n have similar trends, but on the boundaries and further away from the contact their trends can be significantly different (Fig. 4).

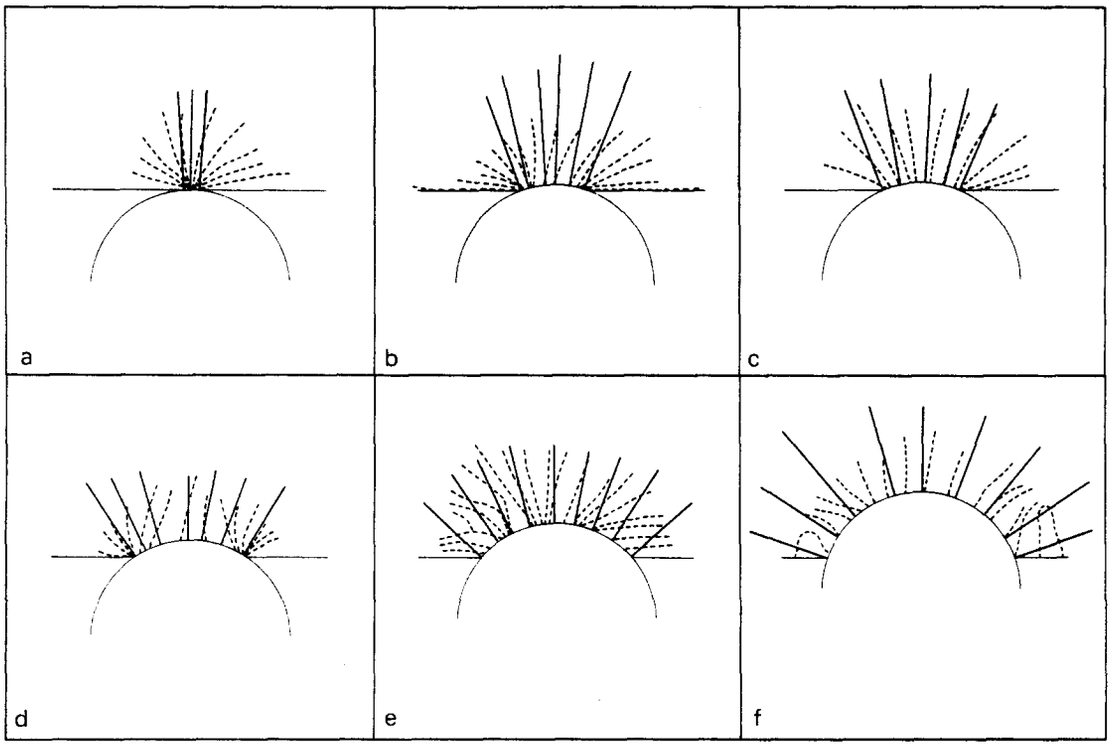

Fig. 4. Trajectories of σ_1, (dashed lines) and σ_n (solid lines) for the six loading configurations (detailed in the section entitled Photoelastic experiments).

Discussion

The isochromatic maxima on the boundaries of the contact zone are probably more pronounced than would exist in natural rocks. This is because of the much lower value for Young's Modulus for araldite than for limestone (2.75×10^3 MPa as compared with a value as high as 6.2×10^4 MPa).

It is very noticeable in pitted pebble conglomerates that for limestone pebbles of similar composition the pebble with the smaller radius of curvature at the contact always penetrates the pebble with the larger radius of curvature. The stress distribution within the less curved, but not necessarily larger, pebble must be different from that in the penetrating pebble.

Hertzian theory predicts (Hertz 1881) the same stress distribution in both bodies around the contact, because the theory is only exactly correct for a surface being a plane in the deformed state. The change can be estimated qualitatively in passing from a plane to a spherical surface, by cutting out the sphere from the plane surface according to Fig. 5 (seen in two dimensions). In the region marked by oblique lines the stress trajectories of σ_1 and σ_2 are almost exactly radial and circular respectively. They are also extensional in this region, and in the contact area σ_1 and σ_2 being positive (compressive) will be decreased in magnitude, whilst σ_3, also being positive, will remain the same; so that $(\sigma_1 - \sigma_3)$ will decrease. Hence the plastic limit, the first fracture and the onset of any dilatant effects will occur in the plane before they occur in the sphere. A similar argument thus applies to bodies of different curvature, the decrease in the stress differences will increase as the radius of curvature increases. Although along the contact surface the stresses will be equal and opposite, within and on the unloaded boundary of the pebble with the higher radius curvature the stress gradients will be higher than on the other pebble. Any diffusional mass transfer will preferentially occur in the pebble with the larger radius of curvature.

Figure 6 shows the stress distribution along the line AB normal to, and through the centre of, the contact between the disc and the plane. σ_{zz}, $(\sigma_{zz} - \sigma_{xx})$, σ_{xx}, $\bar{\sigma}$ $(= \frac{1}{2}(\sigma_{xx} + \sigma_{zz}))$ and σ_{zx} all have higher values in the plate than in the disc. σ_{zx} is zero at the contact and has its highest value at a small distance along the loading axis within the plate. This result is in agreement with the qualitative assessment made above.

During the initial Hertzian loading very high tensile stresses are produced immediately around the edge of the contact area. The maximum tensile stress (Fig. 1b) is higher than the maximum shearing stress, and for a homogeneous brittle solid a cone crack is produced when the load is high enough. In most circumstances limestone pebbles are not homogeneous and brittle enough to allow the propagation of a cone crack, but it is likely that tensile micro-cracks are nucleated in the surface region of the pebble. Because of the very heterogeneous nature of the stress field around the contact area, any crack that nucleates in the surface layer requires an even higher load before it will propagate further into the rock. Many limestone pebbles do not show signs of tensile cracks produced by initial Hertzian loading or by point loading on opposite sides of the pebble, and it must be concluded that the stresses in these cases were not high enough. If there is a tangential component to the loading then even higher tensile stresses are developed on the 'trailing edge' of the contact area (Hamilton & Goodman 1966).

Shear planes, which have similar curved surfaces to those found from the experiments, are found especially in marl pebbles and pebbles with affected zones (McEwen 1978). Shearing also occurs in quartzite pebbles around the solution pits.

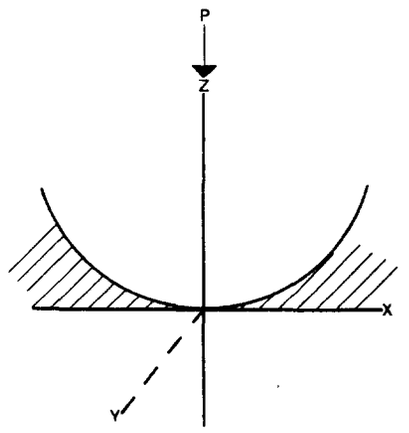

Fig. 5. The contact between a sphere and a semi-infinite plane. In the area marked by the oblique lines (in the XZ plane) the σ_1 trajectories are radial.

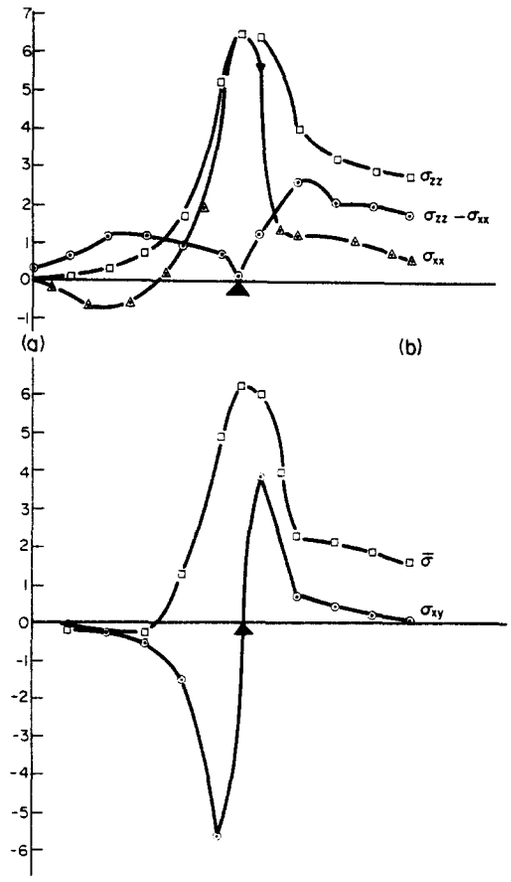

Fig. 6. The stress distribution along line AB, normal to and through the centre of the contact between the disc and the plane. A and B are equidistant from the contact (▲) in the disc and the plane respectively.

Cracks that form along σ_1 trajectories are those which have purely tensile displacements and those that have formed in compression. Over the central part of the solution pit σ_1 and σ_n are sub-parallel (Figs. 4b–f). Tensile cracks that are formed either in response to local stresses around one pit or due to loading on opposite sides of the pebble will thus tend to propagate approximately normal to the pit surface (Figs. 7b–d and 11a). For a small pit, and especially for a pit with low curvatures, tensile cracks will thus be orientated within $\pm x$ to the normal of the base of the pit, where the value of x is in many cases $< 40°$ (Fig. 13).

TYPES OF FRACTURES

Fracturing during the deformation of pitted pebble conglomerates is most common whenever the strain rate is high, the matrix is weak and most of the pebbles are quartzitic. The different types of fracture are:

(1) fractures which occur in the immediate vicinity of a solution pit;
(2) fractures which transect whole pebbles due to point loading;
(3) fractures which transect pebbles and matrix, often with no diffraction at the pebble–matrix boundary.

(1) Fractures which occur in the immediate vicinity of a solution pit usually occur only in the pebble which has suffered volume loss. There are several different types of fracture within this group:

(a) Tensile fractures which form in the surface region of a solution pit in areas where slickensides are developed; they are never more than about 2 μm wide and are confined in limestone pebbles to the outer 1 mm of the pebble. They form at high angles to the pit surface (70–90°) and can be up to 2 mm long. They are usually orientated normal to the slickensides and exhibit only tensile opening displacements normal to their walls.
(b) Tensile fractures which form at lower angles to the slickenside lineation but which are still approximately normal to the solution pit surface. They have similar dimensions to the fractures of group 1(a).
(c) Tensile fractures which form at lower angles to the pit surface, this type of fracture is also commonest where slickensides are present.
(d) Surfaces on which shear displacements have occurred. These are best developed in marl pebbles where ductile shearing occurs on conjugate surfaces and in quartzite pebbles where cataclasis takes place on the shear planes.
(e) Fractures which form along the boundaries between grains and the matrix. They are most important in calcite cemented sandstones and arkose pebbles, and in some cases initiate the collapse of the pebble structure adjacent to the indenting pebble.
(f) Tensile fractures which form at the boundary of the contact area of two pebbles. They only occur in the more brittle pebbles, and when the contact between the two pebbles has a low curvature.

(2) Fractures which transect whole pebbles are often produced by point loading on opposite sides of the pebble. They usually have no shear component along their lengths, and are filled with calcite. They are of two types:

(a) cracks which are related to the local stress field produced by the contact between pebbles and
(b) cracks which were inherited from the rock from which the pebble was formed.

Type 2(a) fractures are commonest in fine-grained limestone pebbles which have suffered large volume losses. These cracks can be up to 100 μm wide, but their usual size range is 12–50 μm. They are commonly straight and occur in groups of almost perfectly parallel cracks with crack densities of up to 30 per cm. They are often orientated to within $\pm 30°$ to the normal of the solution pit, and have strong orientation maxima (Fig. 7). Type 2(b) cracks are commonest in very fine grained (grain size $\leqslant 5$ μm) slightly impure limestones. They are straight, have widths of 8–35 μm, but their orientations do not appear to be related to the solution pit distribution. They also occur in groups of almost perfectly parallel cracks with local densities of up to 45 per cm and have higher overall densities than type 2(a) cracks, up to 35 per cm in cross sections of pebbles, as compared with a maxima of 12.5 per cm for type (a) cracks. They are invariably straighter than type (a) cracks (Fig. 8), and even where they intersect they are not deflected. They are displaced by solution seams which are commonest in the same type of limestone pebbles (Fig. 10d).

(3) Fractures which transect pebbles and matrix. This type of fracture is commonest in conglomerates which are well cemented and where the deformation rate has been high, e.g. on the south side of Rigi, Switzerland, where Cretaceous to Eocene rocks are thrust over the Molasse. They are best developed in conglomerates where the strength of the matrix is similar to that of the pebbles, and are uncommon in quartzite conglomerates with a dominantly calcite cement. Where the conglomerates are well cemented the cracks are not deflected at pebble–matrix boundaries. These cracks are usually infilled with calcite.

Type 1 (a, b, c) fractures

The tensile cracks that form on the surface of solution pits on which sliding has occurred are probably formed because of the high tensile stresses that develop in the surface region of the pit due to sliding.

The fractures that are produced during sliding have been variously described as Hertzian fractures, Riedel shears and fractures produced in compression.

Hertzian fractures

When a tangential force is applied to a specimen by an

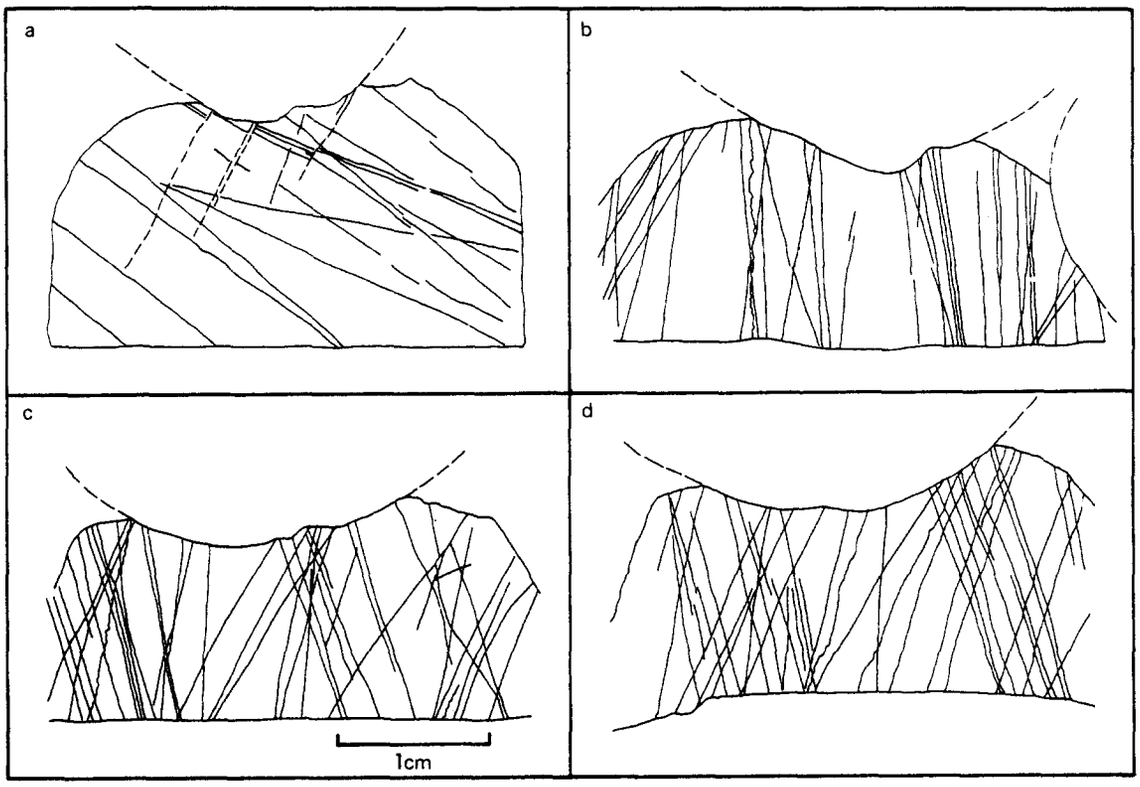

Fig. 7. Fracture patterns in parts of cross-sections of extensively fractured limestone pebbles from the Molasse of the Voreppe Syncline near Grenoble. Most of these fractures are related to the solution pits.

indenter, as in the case of sliding contact, the stress fields (Hamilton & Goodman 1966) and consequent fracture path (Lawn 1967) within the solid become increasingly dependent upon the coefficient of friction at the interface (La Fountain 1975). A change in the coefficient of friction alters the shear traction which modifies the shape of the cracks, such that they become more normal and even obtuse to the surface as the coefficient of friction increases.

Riedel shears

Coulson (1970) has suggested that Riedel shear fracturing causes the development of grooves in a sliding surface. Riedel shears were first described in relation to clay and develop at $\phi/2$ to the direction of shear when ϕ is the angle of internal friction. Riedel shears should thus form at 10–20° to the surface of the solution pit.

Fractures formed in compression

From a study of step structures on slickensides, Gay (1970) suggested that the step formation was partly due to the propagation of cracks away from the plane in a direction parallel to the maximum compressive stress when the stress reaches a critical level (Hoek 1965, p. 65). The theory of the development of cracks in compression was first formulated by Brace & Bombolakis (1963). Cracks in the pit surface are best developed in areas where slickensides also exist, assuming that areas of slickensided surface are where contact occurred between the pebbles. It is in these places on the pit surface where the highest stresses will exist. These tensile cracks will propagate away from the pit surface taking advantage of any suitably aligned planes of weakness such as grain boundaries.

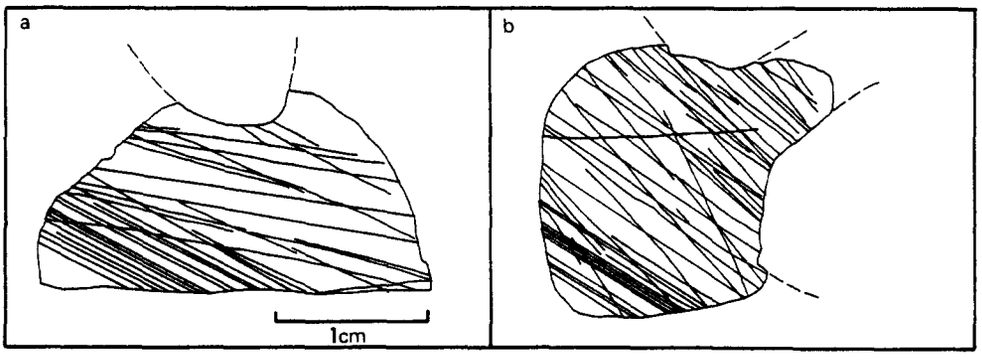

Fig. 8. Fracture patterns in cross-section of limestone pebbles from the Molasse of the St. Egrève Syncline, near Grenoble. Most of the fractures do not appear to be related to the solution pits.

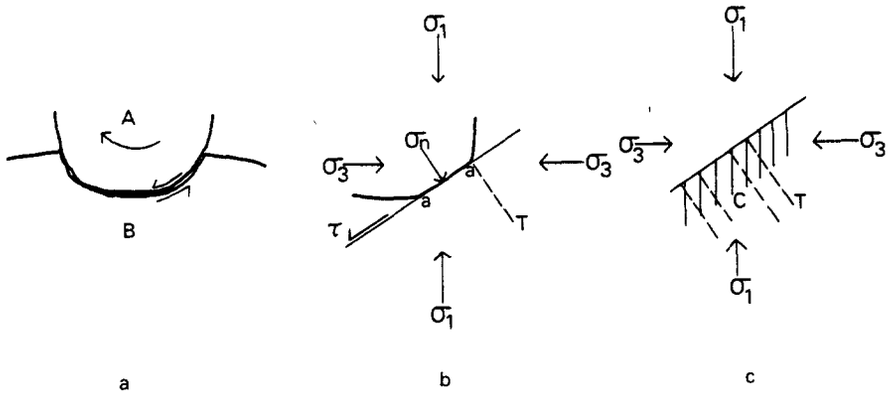

Fig. 9 (a)Two pebbles rotating against each other along the surface of a solution pit. (b) Part of the contact made between the pebbles (aa), σ_1, σ_3 = maximum and minimum principal compressive stresses; σ_n = stress normal to contact plane; τ = shear stress along contact; T probable position of tension crack at trailing edge of contact. (c) Formation of tension cracks parallel to σ_n and parallel to σ_1 in the surface region of the contact.

The tangential stresses are distributed over the area of contact as in Fig. 9(b). Jaeger & Cook (1976, pp. 280–282) give equations of the stresses perpendicular and parallel to the shear plane by considering the theory of friction on a closed Griffith's crack (Hoek & Bieniawski 1965). Very large tensile stresses are produced at points near the trailing edge of the area of contact parallel to the shear plane. Tension cracks may form, theoretically parallel to σ_1, but they will probably propagate along grain boundaries and thus could vary in orientation.

If the coefficient of sliding friction is known, then the theoretical angle of these tension cracks can be calculated assuming the Coulomb criterion of failure. Coefficients of sliding friction (μ_s) for limestone subjected to a normal stress of 200 bars (20 MPa) are probably in the range of $0.8 > \mu_s > 0.3$. The angle (β) between σ_1 and σ_n is given by

$$\beta = \frac{\pi}{2} - \tfrac{1}{2}\tan^{-1}\left(\frac{1}{\mu_s}\right)$$

giving values for β of $64° > \beta > 53°$. The values of the angle between the crack and the pit surface (α) ($= (90 - \beta)$) are $37° > \alpha > 26°$, the largest value of (α) possible in other rocks is about 42°.

When the pebbles slide against each other they do not make contact over the whole surface but on asperities. Equations have been derived for the complete stress field created by a circular sliding contact (Hamilton & Goodman 1966). These equations show that there are large tensile stresses developed in the subsurface region close to the trailing edge of the indenter. They also show that the square root of the second invariant of the stress deviator tensor ($J_2^{1/2}$) also has its maximum value near the trailing edge of the indenter.

The most important parameter which determines the shape of the stress contours is the coefficient of sliding friction (μ_s). Plastic yielding occurs when $(J_2)^{1/2}$ reaches the material yield point in simple shear. With increase in μ_s values of $(J_2)^{1/2}/p_0$ (where p_0 = the maximum pressure at the centre of the contact), reach a value of 0.553 when $\mu_s = 0.5$. For all values of $\mu_s \geqslant 0.27$ the point of maximum yield stress is on the surface.

For brittle materials the appearance of tensile stresses is more important than the value of the yield parameter. Even if the coefficient of friction is zero, one of the principal stresses in the surface is tensile near the edge or the contact. The stress acts in a radial direction. With increase in μ_s the stress distribution becomes unsymmetrical, compressive at the front of the contact and greatly intensified and tensile at the rear. When $\mu_s = 0.5$ the tensile stresses at the rear edge of the contact have increased to equal the compressive stress of the centre. The tensile stress system is very shallow and a tensile crack will propagate, most likely parallel to σ_n and at a high angle to the surface, except if $\mu_s \sim 0$, when the minimum angle between the surface and the crack is about 35°.

Shear fractures (Type 1(d) fractures)

These are best exhibited in marl and quartzite pebbles though the detailed nature of the shearing process is different in the two rock types. They also occur to a lesser extent in pebbles of other compositions which have a high percentage of insoluble residue ($\geqslant 20\%$) and in calcite cemented sandstone pebbles.

They are commonest in marl pebbles because (a) marls are often weak, (b) they are often poorly cemented because of the clays present and (c) they undergo disaggregation relatively easily when calcite is removed from their structure by diffusional mass transfer. Shearing is commonly associated with affected zones which are often best developed in marl pebbles (McEwen 1978). When more than about 20% of the calcite has been removed from the rock, shearing occurs on curved conjugate planes in a similar way to the experimental deformation of clays (Morgenstern & Tchalenko 1967). The direction of shear is normally directed inwards and downwards towards the centre of the solution pit or the affected zone. The shear planes are essentially collapse structures which form in response to the volume loss which occurs during removal of the calcite. The process is probably one of ductile shearing (Odé 1959, Means 1977) (Fig. 10a).

Calcite cemented sandstones and arkoses sometimes suffer shearing around solution pits when the calcite is preferentially removed and the quartz grains rotate and undergo grain boundary sliding as the strength of the rock is reduced (Fig. 10b). The disaggregation process is initiated and enhanced by microcracking between quartz grains and the matrix. Microcracks form along grain boundaries because the different elastic moduli of the grains and the matrix produce differential strains on the grain boundaries when stresses are applied, and because the boundaries between the grains and the matrix will often have the lowest interface boundary strengths. Low boundary strengths are often due to the presence of clays and micas along grain boundaries which prevent good bonding between the grains and the cement. The intragranular fracturing commences near or just outside the contact with the penetrating pebble. There is then a combined effect of calcite removal and crack propagation through the rock. The highest stresses are developed around the margins of the quartz grains, and calcite is most likely to be removed in these positions first. This will increase the chance that cracks will propagate in these regions. When the cement–grain boundaries have become weakened grain rotation occurs in response to the applied stresses.

Slip between grains and cement, and along mutual grain contacts is enhanced by the presence of micas and clays on grain surfaces, because the coefficients of sliding friction are lowered. During this process dilatancy will occur in parts of the affected zone and the influx of more water into the area will make grain boundary sliding even easier.

The whole process can be considered as a transport-controlled or chemically-enhanced creep rupture, or as a fracture enhanced diffusion mass transfer process. Both diffusion and rupture are occurring simultaneously.

Low angle shearing occurs around the contacts between quartzite pebbles (Fig. 1d). In contrast with marl pebbles the shear displacements are often directed away from the centre of the solution pit. The pebbles tend to flatten against each other because the rate of removal of quartz from the pebble contact is not fast enough to accommodate the strain. There is intense granulation along the shear planes.

Type 1(e) fractures

Microcracking of grain boundaries has been discussed in section 1(d) in relation to affected zones and grain boundary sliding in calcite cemented sandstone and arkoses. Grain size has an important effect on the nucleation and growth of cracks. The stress needed for nucleation of cracks increases with decrease in grain size according to the 'Petch relationship' (Lawn & Wilshaw 1975) as the resolved component of the shear stress $\propto d^{-1/2}$, where d is the grain diameter. The resistance to fracture may be intrinsically low along grain boundaries, but the abrupt change in fracture path at each grain will lead to a large reduction in the local mechanical energy release rate, and a tendency to an increased fracture resistance with decrease in grain size.

Grain boundary cracking will be influenced to a great extent by the chemical environment along the boundary, and chemically enhanced creep rupture may occur. The cause of fracture at grain boundaries may be associated with the subcritical extension of an incipient flaw when exposed to a reactive species e.g. H_2O. Grain boundary cracking then becomes an activated process.

Type 1(f) fractures

When the two pebbles are in contact along a surface with a small curvature and the pebbles have very different hardness and elastic moduli, the situation can be approximated by the contact of an elastic stamp on a semi-infinite plane. The approximation holds so long as the stress level does not exceed a critical limit above which the rock will become inelastic and anisotropic, and so long as neither of the rocks is very soft (i.e. marl, shale). Theoretical solutions for this problem have been derived by Love (1929) and Sneddon (1946).

These solutions predict high tensile stresses in a shallow region near the free surface outside the contact area. The tensile stresses attain a maximum value adjacent to the edge of the stamp. The possible failure modes for the rock are:

(1) The formation of a tensile ring crack close to the edge of the stamp where the tensile stresses attain their maximum value. Because most rock has low tensile strength any failure will begin here.
(2) The rock will fail along the contour of the hemispherical region where one of the principal stresses is tensile.

The maximum effective stresses at pebble contacts cannot in many cases be greater than about 20 MPa, because extensive cracking and failure of pebbles at their mutual contacts does not usually occur. It is therefore unlikely that any more than a small tensile ring crack will form. This type of crack is found in some crystalline limestone pebbles at the edge of their contact with a quartzite pebble (Fig. 1b). The tensile crack allows a partial elastic rebound of the surface to occur.

Wagner & Schumann (1971) have shown that for large stamps, the bearing strength of all the rocks tested by them (quartzitic shale, norite, marble and sandstone) were about four times the respective uniaxial compressive strengths. The bearing strengths varied from about 0.38 GPa for sandstone to 0.9 GPa for quartzite. Except for small areas on the contact surface where asperities are in contact, or where rapid deformation of the conglomerate occurs, e.g. beneath an overthrust mass, these stresses are never realised. The affected zones around indenting pebbles are therefore not due to an initial failure of the rock around the indentation and then subsequent removal of calcite or quartz.

Type 2(a) fractures

Larger tensile fractures which transect pebbles are often

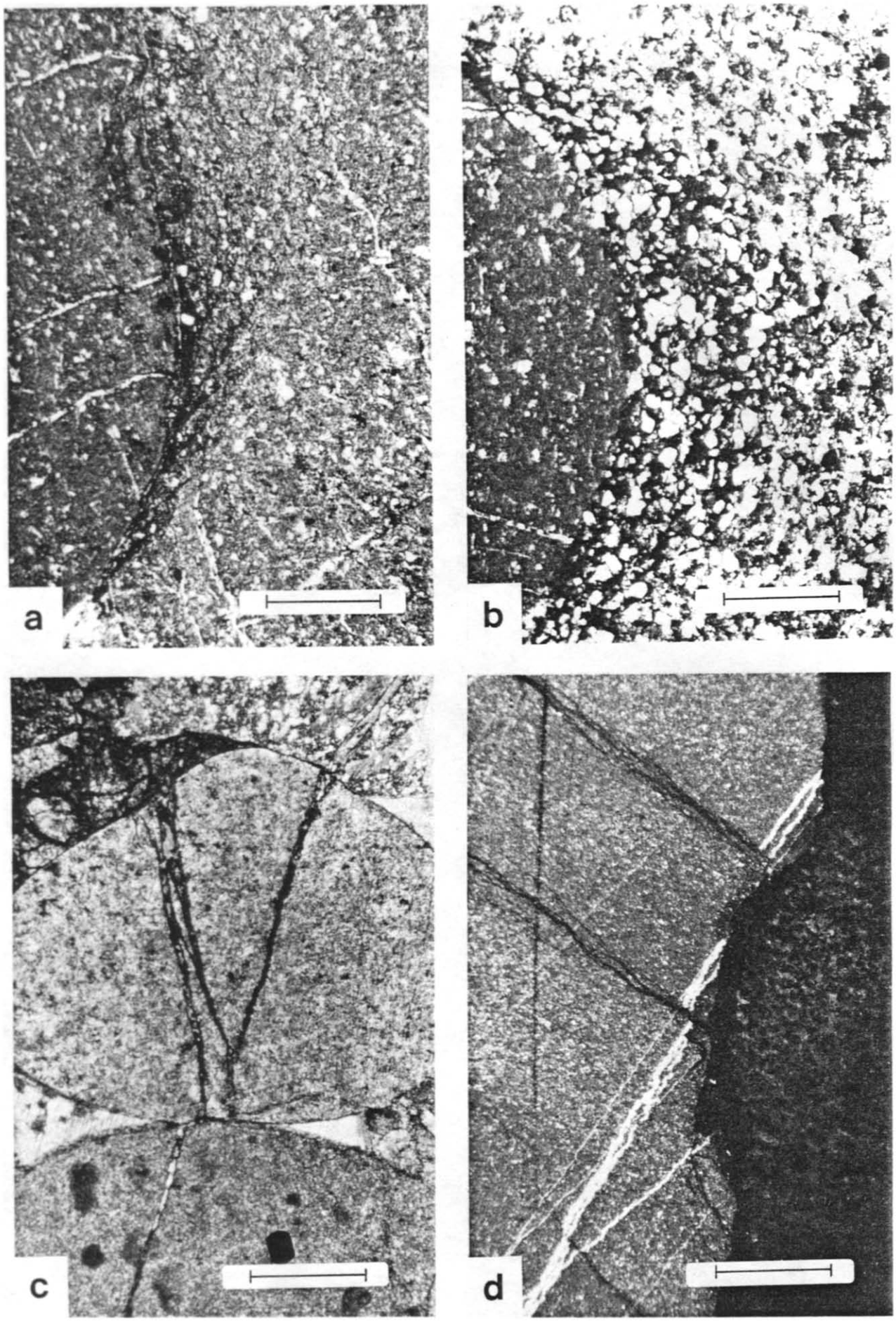

Fig. 10(a). Curved ductile shear planes formed in marl pebbles around their mutual contact, Kalknagelfluh, Stänis, Switzerland. Scale bar = 1 mm. (b) Disaggregation zone in calcite cemented arkose pebble produced by the indentation of a limestone pebble, Kalknagelfluh, Stänis, Switzerland. Scale bar = 1 mm. (c) Two calcite-filled tension cracks formed in arkose pebble due to point loading on opposite sides of the pebble, Molasse, Proveysieux Syncline, France. Scale bar = 0.5 mm. (d) Calcite-filled tension cracks, truncated by solution seams normal to the cracks, around a solution pit in a limestone pebble, Molasse, Proveysieux Syncline, France. Scale bar = 1.0 mm.

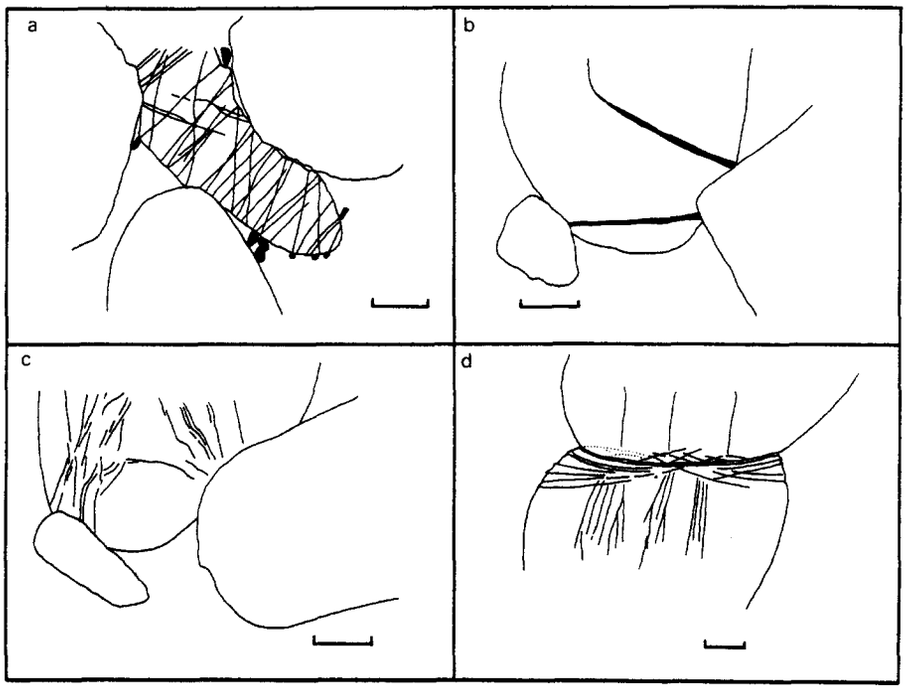

Fig. 11. (a) Multiple cracking of limestone pebble. Most of the cracks are at high angles to the pebble contacts. (b) Large calcite-filled tension cracks formed at the edges of the contact between two crystalline limestone pebbles, Bunte Nagelfluh, Rigi. (c) Thin crush zones formed around the contacts between quartzite pebbles, Mieres Conglomerate, Spain. (d) Shear cracks formed at low angles and tension cracks at high angles to the contact between two quartzite pebbles, Mieres Conglomerate, Spain. All scale bars = 1 mm.

due to approximately point loading on opposite sides of the pebble. Fractures propagate across the whole pebble because the high stress concentrations due to the point loads produce high tensile stresses in the region along their line of contact (Fig. 10c). Theoretically, a tensile fracture should initiate just below the loaded edge (when the Griffith crack criterion is applied) but frictional restraint on the load contact surface will probably make all stresses in this region compressive. The exact state of stress around the loaded areas is therefore not known accurately, and there may be small shear fracture precursors around the contact areas before ultimate tensile failure occurs (Fairhurst 1964, Gallagher *et al.* 1974).

As previously noted by Gallagher *et al.* (1974) fractures in both cemented and uncemented aggregates develop parallel σ_1 trajectories and lie along lines which are the loci of the greatest values of the maximum stress difference. This implies that an extension fracture criterion is applicable and that the fractures have no related shear components.

Tensile fractures that develop around pebble contacts when the solution pit has formed exhibit more complex patterns, because the stress state is more complex than for approximately point loading. Some of these tensile fractures are initiated by rotation between the pebbles, others are associated with solution pit surfaces which have high radii of curvature. The loading configuration is then similar to the theoretical situation of a distributed load on the edge of a semi-infinite plate. The contours of σ_1 beneath a large part of the loaded body in the region close to the contact are within ± 25–$30°$ to the normal to the loaded surface and large tensile stresses normal to the direction of loading are produced around the edges of the contact. Tensile cracks orientated within this range are found around solution contacts in the larger limestone pebbles.

These tensile cracks are often concentrated near the boundaries of the solution pit where the largest tensile stresses would be expected. They do not follow smooth curves, as predicted from the form of the σ_1 trajectories in Fig. 12 because (a) the pebble is not a semi-infinite body and (b) the crack orientations are also determined by the positions of the other solution pits on the pebble. Figure 7 shows a cross section of a limestone pebble containing numerous tensile fractures. It can be seen that (a) the tensile cracks are orientated within $\pm 30°$ to the normal of the base of the solution pit, (b) cracks are straight, (c) there are higher crack densities around the edges of the solution pit and (d) crack orientations exhibit two distinct maxima at $+12°$ and $-22°$ to the base of the pit (Fig. 13).

Type 2(b) fractures

These cracks are presumed to have been produced in the limestone before it was eroded to produce the pebble. They are often visible in almost undeformed limestones in

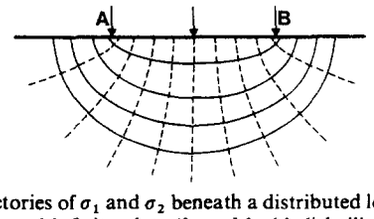

Fig. 12. Trajectories of σ_1 and σ_2 beneath a distributed load on the edge of a semi-infinite plate (from Muskhelishvili 1953).

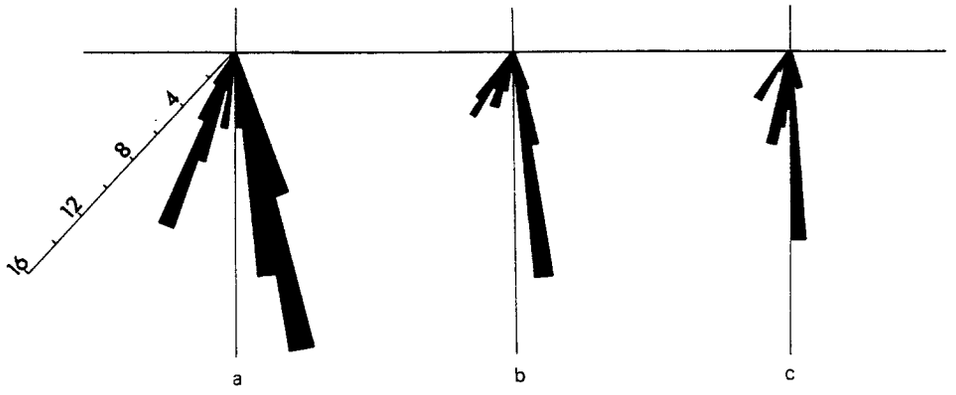

Fig. 13. Orientations of tension cracks around solution pits in cross sections of limestone pebbles from the Proveysieux Syncline, France. Most cracks lie within ±30° to the normal to the base of the pit.

the external zones of the Western Alps e.g. around Castellane, especially on weathered surfaces where they stand proud.

Fractures that transect pebbles and matrix

This type of fracture is common in conglomerates which lie close to major faults and where the strain rate in the conglomerate has been high. They are particularly common in the Molasse near the Frontal Alpine Thrust. There are two types:

(a) In places where the conglomerates are very well cemented with a dominantly calcite cement there is often little difference in the values of the elastic moduli between the pebbles and the matrix. The positions of the fractures (in these cases) are generally not determined by the pebble–matrix boundaries. This is because high stress concentrations are not produced where pebbles are in contact, but in the central parts of the pebbles. The fracture orientations are therefore determined by the bulk stress system applied to the conglomerate. Examples of this type of fracture are found near the overthrust Säntis Nappe, where planar calcite-filled tensional fractures cut through pebbles and matrix, and are aligned normal to the direction of overthrusting, and

(b) Where the strength of the pebble–matrix bond is not as high; and where there is a large difference in the mineralogy between the pebbles and the matrix, the fractures are often deflected around pebble boundaries. This type of fracture is often formed earlier than type (a) fractures when the conglomerate is not so well cemented. Examples of this type of fracture are common on Rigi, Switzerland.

Both types of fracture exhibit dominantly tensile displacements and many were open fissures with the infilling calcite showing structures associated with vug growth.

Brittle deformation in the matrix

The previous discussion has been concerned with cracks that form in the conglomerate pebbles, but the matrix also suffers brittle deformation. Although in many cases the largest loads are supported by the pebble framework with subsequently smaller loads on the matrix, as soon as pebble movement occurs due to pitting, fracturing or rotation, some of the load will be transferred to the matrix. The matrix then behaves just like a deforming sandstone and the fracture patterns are dependent on the mineralogy of the grains, the composition of the cement, the strain rate and the orientations of the bulk principal stresses. Because the stress states within the matrix were very complex, and continually changing during the deformation, it is very difficult to say anything constructive regarding the fracture patterns within it in relation to the deformation of the conglomerate. As expected, fractures are best developed in matrices made up of quartz grains with a calcite cement, but the fracture pattern is related to the stress inhomogeneities on the scale of a few grains and cannot be related in any simple way to movements that have occurred between pebbles. The general distribution of fractures in the matrix is in agreement with previous predictions of fracture patterns by Gallagher *et al.* (1974), Hoshino & Koide (1970), Friedman (1963) etc.

CONCLUSIONS

Photoelastic experiments which model the progressive pitting of one pebble by another, and theoretical results calculated from the loading of rigid and elastic bodies, can be used to predict the fracture patterns that are produced in pitted pebble conglomerates. Fractures associated with local stress concentrations around pebble contacts are shown to be either due to the high tensile stresses which are developed in these regions, or to shearing along planes of weakness in the rock. Fractures which transect pebbles are shown to be dominantly tensile in character.

The results derived from the photoelastic experiments are only valid if the pebble acts as a continuum. For marl pebbles, which do not exhibit very brittle behaviour but instead deform by simultaneous shearing and diffusional mass transfer, the experimental stress distributions will only be very approximate. For brittle crystalline lime-

stone and quartzite pebbles the experimental results are probably much closer to nature.

This study emphasises the importance of brittle deformation features in rocks deformed at low temperatures. Studies by ceramicists and geologists on quartz, glass and similar materials has shown that it may be possible to estimate the stresses involved during the failure of quartz bearing sediments (Norton & Atkinson in press). It may thus be possible to determine the stress distribution within such rocks from a study of their fracture patterns.

Acknowledgements—This paper is based on part of a Ph.D. thesis submitted to the University of Leeds in 1977, and a grant from N.E.R.C. is gratefully acknowledged. I would like to thank Prof. J. G. Ramsay for guidance during the research.

This paper is published with permission of the Director of the Institute of Geological Sciences (Natural Environmental Research Council).

REFERENCES

Brace, W. F. & Bombolakis, E. G. 1963. A note on brittle crack growth in compression. *J. geophys. Res.* **68**, 3709–3713.

Coulson, J. H. 1970. The effects of surface roughness on the shear strengths of joints in rock. Technical Report MRD-2-76, Missouri River Division, Corps of Engineers, Omaha, 1–283.

Fairhurst, C. 1964. On the validity of the 'Brazilian' test for brittle materials. *Int. J. Rock. Mech. Min. Sci.* **1**, 535–546.

Friedman, M. 1963. Petrofabric analysis of experimentally deformed calcite-cemented sandstones. *J. Geol.* **71**, 12–37.

Gallagher, J. J., Friedman, M., Handin, J. & Sowers, G. M. 1974. Experimental studies relating to microfracture in sandstones. *Tectonophysics* **21**, 203–247.

Gay, N. 1970. The formation of step structures on slickensided shear surfaces. *J. Geol.* **78**, 523–532.

Hamilton, G. M. & Goodman, L. E. 1966. The stress field created by a circular sliding contact. *J. appl. Mech.* **33**, 371–384.

Hertz, H. 1881. Gessammelte Werke. *J. Math.* (Crelle's J.) **92**, 156–174.

Hoek, E. 1965. Rock fracture under static stress conditions. Council Sci. Indus. Res. Rept. MEG 383: Pretoria, Natl. Mech. Eng. Res. Inst.

Hoek, E. & Bieniawski, Z. T. 1965. Brittle fracture propagation in rock under compression. *Int. J. Fracture Mech.* **1**, 137–155.

Hoshino, K. & Koide, H. 1970. Process of deformation of the sedimentary rocks. In: *Proc. of the 2nd Int. Cong. R. Mech.* **1**, papers 2–13.

Jaeger, J. C. & Cook, N. G. W. 1976. *Fundamentals of Rock Mechanics* (2nd ed.) Methuen and Co., London.

Kuske, A. & Robertson, G. 1974. *Photoelastic stress analysis.* J. Wiley and Sons, New York.

La Fountain, L. J., Swain, M. V. & Jackson, R. E. 1975. Origin of macroscopic wear grooves generated during sliding friction experiments. *Int. J. Rock Mech. Min. Sci.* **12**, 367–371.

Lawn, B. R. 1967. Partial cone crack formation in a brittle material loaded with a sliding spherical indenter. *Proc. R. Soc.* **299A**, 307–319.

Lawn, B. R. & Wilshaw, T. R. 1975. Indentation fracture: principles and applications. *J. mater. Sci.* **10**, 1049–1081.

Love, A. E. H. 1929. The stress produced in a semi-infinite solid by pressure on part of the boundary. *Phil. Trans. R. Soc.* **228A**, 377–420.

McEwen, T. J. 1977. Pressure solution processes in rocks. Unpublished Ph.D. thesis, University of Leeds.

McEwen, T. J. 1978. Diffusional mass transfer processes in pitted pebble conglomerates. *Contr. Miner. Petrol.* **67**, 405–415.

Means, W. D. 1977. A deformation experiment in transmitted light. *Earth Planet. Sci. Lett.* **35**, 169–179.

Morgenstern, N. R. & Tchalenko, J. 1967. Microscopic structures in kaolin subjected to direct shear. *Geotechnique* **17**, 309–328.

Muskhelishvili, N. I. 1953. *Some Basic Problems of the Mathematical Theory of Elasticity.* 4th. ed., English Trans., Noordhoff, Groeningen.

Norton, M. G. & Atkinson, B. J. in press. Stress dependent morphological features on fracture surfaces of quartz and glass. *Tectonophysics.*

Odé, H. 1960. Faulting as a velocity discontinuity in plastic deformation. In: *Rock Deformation*; (edited by Griggs, D. T. & Handin, J.). *Mem. geol. Soc. Am.* **79**, 293–322.

Sneddon, I. N. 1946. Boussinesq's problem for a flat ended cylinder. *Proc. Cambridge Phil. Soc.* **42**, 29–39.

Wagner, H. & Schumann, E. H. R. 1971. The stamp-load bearing strength of rock — An experimental and theoretical investigation. *Rock Mechanics* **3**, 185–207.